fermentation

MDPI

Article

Highly Active Astaxanthin Production from Waste Molasses by Mutated *Rhodosporidium toruloides* G17

Tuyet Nhung Tran [1], Ngoc-Tri Tran [1], Thu-Anh Tran [1], Dinh-Chuong Pham [1], Chia-Hung Su [2], Hoang Chinh Nguyen [3,*], Colin J. Barrow [3,*] and Dai-Nghiep Ngo [4,*]

1 Faculty of Applied Sciences, Ton Duc Thang University, Ho Chi Minh City 700000, Vietnam
2 Department of Chemical Engineering, Ming Chi University of Technology, New Taipei City 24301, Taiwan
3 School of Life and Environmental Sciences, Deakin University, Geelong, VIC 3216, Australia
4 Faculty of Biology and Biotechnology, University of Science, Vietnam National University-HCM, Ho Chi Minh City 700000, Vietnam
* Correspondence: hoang.n@deakin.edu.au (H.C.N.); colin.barrow@deakin.edu.au (C.J.B.); ndnghiep@hcmus.edu.vn (D.-N.N.)

Abstract: Astaxanthin is increasingly attracting commercial interest for its application in the nutraceutical and pharmaceutical industries. This study aimed to produce astaxanthin from molasses with our newly mutated strain of *Rhodosporidium toruloides* G17 and to evaluate biological activities of the produced astaxanthin. To maximize the astaxanthin yield, the response surface methodology was used so as to optimize the culture conditions. A maximum astaxanthin yield of 1262.08 ± 14.58 μg/L was achieved by growing *R. toruloides* G17 in a molasses-based medium containing 49.39 g/L reducing sugar, 1.00 g/L urea, 4.15 g/L $MgSO_4 \cdot 7H_2O$, and 10.05% inoculum ratio. The produced astaxanthin was then purified and studied for its antioxidant and anticancer activities. This compound exhibited 123-fold higher antioxidant activity than α-tocopherol, with an IC_{50} value of 0.97 ± 0.01 μg/mL. The astaxanthin also showed a potent inhibitory ability against the following three cancer cell lines: HeLa, A549, and MCF7, with IC_{50} values of 69.07 ± 2.4 μg/mL, 55.60 ± 2.64 μg/mL, and 56.38 ± 4.1 μg/mL, respectively. This study indicates that astaxanthin derived from our newly mutated *R. toruloides* G17 is a promising anticancer and antioxidant agent for further pharmaceutical applications.

Keywords: astaxanthin; molasses; optimization; antioxidant; anticancer

Citation: Tran, T.N.; Tran, N.-T.; Tran, T.-A.; Pham, D.-C.; Su, C.-H.; Nguyen, H.C.; Barrow, C.J.; Ngo, D.-N. Highly Active Astaxanthin Production from Waste Molasses by Mutated *Rhodosporidium toruloides* G17. *Fermentation* **2023**, *9*, 148. https://doi.org/10.3390/fermentation9020148

Academic Editor: Mekala Venkatachalam

Received: 9 January 2023
Revised: 23 January 2023
Accepted: 29 January 2023
Published: 2 February 2023

1. Introduction

In recent decades, bioactive compounds from natural sources have received growing interest due to their effectiveness and positive effect on human health, especially antioxidant and anticancer activities [1]. Particularly, astaxanthin, a xanthophyll carotenoid, possesses potential antioxidant and inhibitory effects against a variety of cancers including gastric, bladder, lung, colon, breast, and hepatocellular carcinoma [1,2]. In addition, astaxanthin exhibits anti-inflammatory, anti-apoptotic, antidiabetic, cardioprotective, and immune modulation characteristics [3,4]. Because of such health benefits, studies have been increasingly focusing on developing efficient methods for producing astaxanthin.

Astaxanthin is primarily produced industrially using chemical synthesis. Synthetic astaxanthin accounts for 95% of the total global market of astaxanthin products [5] and is commonly used for pigmentation in the aquaculture sector [3]. However, the production of astaxanthin using chemical synthesis has negative environmental effects and its use for human applications raises food safety concerns. Consequently, the production of astaxanthin through biological processes has received considerable attention, as a variety of microorganisms can biosynthesize astaxanthin [6,7]. Different microorganisms such as bacteria [8], microalgae [9], and yeast [10] have been investigated for their ability to biosynthesize astaxanthin. However, the industrial biosynthesis of astaxanthin remains limited due to low astaxanthin productivity and high production costs [10]. Therefore,

significant efforts have been made to identify new microbial candidates for astaxanthin production and to develop efficient methods for its production [11,12].

The red yeast *Rhodosporidium toruloides* has been reported as one of the most important sources of carotenoids due to its high biomass accumulation and high growth rate. *R. toruloides* can reach a biomass productivity of up to 6.84 g/L within 4 days of cultivation while microalgae require more than 10 days of cultivation to reach the biomass yield of 0.028–0.7 g/L [13–15]. Recently, we isolated new *R. toruloides* strains for astaxanthin production [16]. To further improve astaxanthin accumulation, we successfully attained an *R. toruloides* mutant (G17) using a gamma irradiation mutagenesis [14]. This gamma-induced mutant is a promising candidate for astaxanthin production. However, neither the cultivation of this strain using waste materials as a cheap carbon source, nor the biological activity of astaxanthin produced by this strain, have been investigated.

Molasses (a by-product of sugar production) has been reported as a suitable low-cost medium for the cultivation of different microorganisms (e.g., microalgae and bacteria) as this waste is a rich source of micronutrients (Mg^{2+}, Ca^{2+}, K^{+}), organic compounds (monosaccharides, protein, lactic acids, glutamic acids, aspartic acids), nitrogen, and phosphorous [17–19]. Therefore, this study investigated the use of waste molasses as a cheap carbon source for growing *R. toruloides* G17. The response surface methodology (RSM) was used to optimize the culture conditions (reducing sugar concentration, urea concentration, mineral concentration, inoculum ratio) used for maximizing the astaxanthin yield. The produced astaxanthin was then extracted, purified, and studied for its anticancer and antioxidant activities.

2. Materials and Methods

2.1. Materials

Molasses (73°Brix) was obtained from Bien Hoa sugar factory (Bien Hoa, Vietnam). Astaxanthin, 2,2-diphenyl-1-picrylhydrazyl (DPPH), 3-5-dinitrosalicylic acid (DNS), α-tocopherol, and 3-(4,5-dimethylthiazol-2-yl)-2,5-diphenyltetrazolium bromide (MTT) were provided by Sigma-Aldrich (Saint Louis, MO, USA). Dimethyl sulfoxide (DMSO), petroleum ether, acetone, and n-hexane were obtained from Sigma-Aldrich (Singapore). Fetal bovine serum (FBS), antibiotics, Dulbecco's Modified Eagle Medium/Nutrient Mixture F12 (DMEM/F12), and DMEM were provided by Gibco (Waltham, MA, USA).

2.2. Inoculum Preparation

The strain used was gamma-mutated *R. toruloides* G17, which was obtained from our previous study [14]. It is a wild-type strain isolated from a water sample collected in Ba Ria-Vung province (Vietnam). The strain was maintained on agar plates containing Hansen medium (50 g/L glucose, 10 g/L peptone, 4 g/L $MgSO_4 \cdot 7H_2O$, 3 g/L KH_2PO_4, and 20 g/L agar) and renewed every two weeks. The culture inoculum was prepared by growing *R. toruloides* G17 in Hansen broth for 24 h and used for further experiments.

2.3. Optimization of Growth Conditions

Molasses was hydrolyzed by sulfuric acid using a previously reported method [20]. The resulting hydrolysate was then used for the cultivation of *R. toruloides* G17. The yeast strain was grown in 250 mL Erlenmeyer flasks containing 100 mL of the molasses hydrolysate-based medium (molasses hydrolysate, urea, and $MgSO_4 \cdot 7H_2O$) at 30 °C for 4 d with shaking at 200 rpm. To maximize the astaxanthin yield, a central composite design (CCD) with five levels and four factors was employed to optimize the culture conditions. The four factors (input variables) included the concentration of reducing sugar in molasses hydrolysate (X_1), urea concentration (X_2), $MgSO_4 \cdot 7H_2O$ concentration (X_3), and inoculum ratio (X_4). Table 1 displays the coded and actual values of four input variables. After the cultivation was completed, the culture was centrifugated at 4000× rpm for 5 min. The cell pellets were then collected, washed twice with distilled water, and dried at 60 °C to a constant weight to measure the cell mass. The dried biomass was then used for

determination of the astaxanthin yield [14,16]. The relationship between the astaxanthin yield (measured response, Y, g/L) and the culture conditions was established by the following equation:

$$Y = \beta_0 + \sum_{i=1}^{4} \beta_i X_i + \sum_{i=1}^{4} \beta_{ii} X_i^2 + \sum_{i=1}^{3} \sum_{j=2}^{4} \beta_{ij} X_i X_j \quad (1)$$

where β_0, β_i, β_{ij}, and β_{ii} are the intercept, linear, interaction, and quadratic coefficients, respectively. Minitab 19 (Minitab Inc., State College, PA, USA) was applied to perform an analysis of variance (ANOVA) and regression analysis to determine the model significance and model parameters. The developed model was then used to determine the optimal conditions for obtaining the maximum astaxanthin yield.

Table 1. Input variables for RSM model.

Variables	Symbols	Variable Levels				
		−2	**−1**	**0**	**1**	**2**
Reducing sugar concentration (g/L)	X_1	30	40	50	60	70
Urea concentration (g/L)	X_2	0.5	0.75	1.0	1.25	1.5
$MgSO_4 \cdot 7H_2O$ concentration (g/L)	X_3	1.0	2.5	4.0	5.5	7.0
Inoculum ratio (%)	X_4	5.0	7.5	10.0	12.5	15.0

2.4. Determination of Reducing Sugar Content

The content of reducing sugars in molasses and molasses hydrolysate was determined using the DNS method [21,22]. Briefly, samples were mixed with an equal volume of DNS reagent, heated at 90 °C for 10 min, and then cooled to room temperature. The absorbance of the mixture was then determined at 540 nm using a V-730 UV-Vis spectrophotometer (Jasco, Portland, OR, USA). Glucose was used as a standard to calculate the reducing sugar content in the sample.

2.5. Determination of Astaxanthin Content

Astaxanthin content was determined using the methods reported by An et al. [23] and Fang and Cheng [24] with some modifications. Dried cells (0.2 g) were homogenized in 3 mL of DMSO for 30 min. The DMSO extract was then obtained by centrifuging the mixture at 4000× rpm for 5 min and removing the solid residues. The residues were then extracted 3 times with 5 mL of acetone to obtain all pigments. The acetone and DMSO extracts were combined, mixed with petroleum ether (1:2, v/v), 20% NaCl solution (5 mL), distilled water (10 mL), and placed at room temperature for phase separation. The petroleum ether extract containing astaxanthin was then collected and the absorbance was measured at 468 nm using a V-730 UV-Vis spectrophotometer (Jasco, Portland, OR, USA). Astaxanthin content was then calculated as follows [14]:

$$Astaxanthin\ content\ (\mu g/g) = \frac{A_{468} \times V \times 10^4}{A_{1cm}\ \% \times M} \quad (2)$$

$$Astaxanthin\ yield\ (\mu g/L) = \frac{Astaxanthin\ content\ (\mu g/g) \times M}{Volume\ of\ culture\ (L)} \quad (3)$$

where A_{468}, $A_{1\ cm}$ %, V, and M are the sample absorbance at 468 nm, the absorbance of 1% (w/v) astaxanthin solution in petroleum ether (cuvette width of 1 cm, $A_{1\ cm}$ % = 2100), the total volume of petroleum ether extract (mL), and the total dry weight of yeast biomass (g), respectively.

2.6. Astaxanthin Purification

The crude extract of astaxanthin was subjected to a petroleum ether–acetone–water system to obtain the carotenoids-rich upper layer. The carotenoids-rich extract was then loaded onto a silica gel 60 (50 g, 230–400 µm, Merck, Singapore) column and eluted with n-hexane:acetone (4:1, *v*/*v*) to fractionate the extract and purify astaxanthin. Subsequently, three fractions (A1, A2, and A3) were obtained and analyzed using thin-layer chromatography (TLC) (Silica gel F254 TLC plate, Merck, Singapore). Astaxanthin in each fraction was then identified by comparing its R_f value with the R_f value of the astaxanthin standard.

2.7. Antioxidant Activity Determination

The antioxidant activity of astaxanthin was investigated using the DPPH radical scavenging activity assay described by Sánchez-Moreno et al. [25] with slight modifications. Serial dilutions of astaxanthin (0.25–1.25 µg/mL) were prepared in DMSO. Each dilution (1 mL) was then mixed with 1 mL of the DPPH solution (0.2 mM in DMSO) and placed at 37 °C for 30 min in the dark. The absorbance of the mixture was then determined at 517 nm using a V-730 UV-Vis spectrophotometer (Jasco, Portland, OR, USA). The DPPH radical scavenging activity was calculated as follows:

$$DPPH\ scavenging\ activity\ (\%) = \frac{(A_0 - a_x) - A}{A_0} \times 100 \quad (4)$$

where A, A_0, and a_x are the absorbances of the extracted astaxanthin, the DPPH solution (0.02 mM in DMSO) without astaxanthin, and the extracted astaxanthin without DPPH, respectively. The percentage of DPPH inhibition versus the sample concentration was then plotted to determine the concentration required for a 50% inhibition of DPPH (IC_{50}).

2.8. Cell Culture

Normal kidney cell line HK2, human cervical cancer cell line HeLa, human lung cancer cell line A549, and human breast cancer cell line MCF7 were provided by the American Type Culture Collection (Rockville, MD, USA). Normal HK2 cells were cultivated in DMEM/F12 supplemented with 10% FBS, 5 ng/mL human recombinant epidermal growth factor (Gibco, Waltham, MA, USA), and 1% antibiotics (100 g/mL streptomycin and 100 U/mL penicillin). Cancer cells (HeLa, A549, and MCF7) were grown in DMEM supplemented with 10% FBS and 1% antibiotics (100 µg/mL streptomycin and 100 U/mL penicillin). All cell lines were incubated in a humidified 5% CO_2 incubator at 37 °C.

2.9. MTT Assay

An MTT assay was used to determine cell viability [26]. To facilitate cell attachment, the cell lines (100 µL) were seeded at 8×10^3 cells per well in a 96-well plate for 24 h at 37 °C in a humidified environment of 5% CO_2. Cells were subsequently treated with different concentrations of extracted astaxanthin (10–100 µg/mL) for 72 h before the addition of 10 µL of MTT solution (5 mg/mL) and incubating for 4 h. The supernatant was decanted and 100 µL of DMSO was added to each well for formazan solubilization. The absorbance was then measured at 570 nm using an Envision microplate reader (Perkin Elmer, Waltham, MA, USA). The cell viability was then calculated as follows:

$$Cell\ viability\ (\%) = \frac{Absorbance\ of\ the\ treated\ samples}{Absorbance\ of\ the\ control\ (untreated\ samples)} \times 100 \quad (5)$$

2.10. Statistical Analysis

The antioxidant and anticancer activities were observed in triplicate and the data were presented as mean ± standard deviation (SD). ANOVA with the least significant (LSD) test was conducted to statistically analyze these data using Minitab 19 (Minitab Inc., State College, PA, USA).

3. Results and Discussion

3.1. RSM Model for The Optimization of Culture Conditions

This work used molasses as a cheap carbon source for growing *R. toruloides* G17. To maximize the astaxanthin yield, a CCD-RSM model was used to examine the influence of the culture parameters (reducing sugar concentration, urea concentration, $MgSO_4 \cdot 7H_2O$ concentration, inoculum ratio) on the astaxanthin accumulation and then optimize the culture conditions. Table 2 shows the experimental design matrix for the cultivation of *R. toruloides* G17 and the resulting astaxanthin yield. A low coefficient of variance (CV = 2.85%) was obtained for the central experiments (runs 25–31), indicating the reproducibility and desirable accuracy of the experiments. Thus, the model was then established to express the relationship between the astaxanthin yield and culture conditions as follows:

$$\begin{aligned} Y = 1245 - 15.61X_1 \quad & -0.06X_2 + 18.6X_3 + 3.45X_4 - 182.99X_1^2 - 105.02X_2^2 \\ & -108.43X_3^2 - 107.22X_4^2 - 38.6X_1X_2 - 14.21X_1X_3 \\ & -16.62X_1X_4 - 7.06X_2X_3 + 35.26X_2X_4 + 12.1X_3X_4 \end{aligned} \quad (6)$$

Table 2. Experimental design of the RSM-CCD model and experimental results.

Run	Variables				Astaxanthin Yield (μg/L)	
	X_1	X_2	X_3	X_4	Experimental	Predicted
1	−1	−1	−1	−1	761.27	739.10
2	1	−1	−1	−1	792.65	780.25
3	−1	1	−1	−1	784.20	759.78
4	1	1	−1	−1	665.33	646.53
5	−1	−1	1	−1	825.50	794.65
6	1	−1	1	−1	783.58	778.95
7	−1	1	1	−1	782.38	787.09
8	1	1	1	−1	639.37	616.99
9	−1	−1	−1	1	651.44	618.02
10	1	−1	−1	1	734.84	725.67
11	−1	1	−1	1	779.57	779.74
12	1	1	−1	1	757.95	732.99
13	−1	−1	1	1	707.63	721.97
14	1	−1	1	1	804.15	772.77
15	−1	1	1	1	898.87	855.46
16	1	1	1	1	734.14	751.85
17	−2	0	0	0	506.90	544.28
18	2	0	0	0	458.95	481.83
19	0	−2	0	0	790.36	825.07
20	0	2	0	0	799.28	824.83
21	0	0	−2	0	731.66	774.11
22	0	0	2	0	830.71	848.52
23	0	0	0	−2	773.91	809.24
24	0	0	0	2	798.10	823.03
25	0	0	0	0	1221.52	1245.03
26	0	0	0	0	1295.59	1245.03
27	0	0	0	0	1282.52	1245.03
28	0	0	0	0	1241.34	1245.03
29	0	0	0	0	1201.03	1245.03
30	0	0	0	0	1214.55	1245.03
31	0	0	0	0	1258.63	1245.03

ANOVA was conducted to evaluate the established model shown in Equation (6). As shown in Table 3, the model had an extremely low p value (<0.001), indicating that the developed model was statistically significant at the 95% confidence level. Moreover, the coefficient of determination (R^2) was high (98.53%), signifying excellent correlation between the predicted and experimental values. Therefore, the established model could

provide a reliable prediction. The t test was also performed to evaluate the significance of model parameters. As can be seen from Table 4, small p values (<0.05) were observed for the following factors: linear coefficient of $MgSO_4 \cdot 7H_2O$ concentration (X_3), all quadratic coefficients of reducing sugar concentration (X_1^2), urea concentration (X_2^2), $MgSO_4 \cdot 7H_2O$ concentration (X_3^2), inoculum ratio (X_4^2), two interaction coefficients (X_1X_2, and X_2X_4), and the intercept. These small p values indicate that these parameters were significant factors in the cultivation of *R. toruloides* G17. The developed model was then used to obtain optimal conditions for maximizing the astaxanthin yield.

Table 3. ANOVA for the RSM model.

Source	DF [b]	SS [b]	MS [b]	*F*-Value	*p*-Value
Model [a]	14	1,582,917	113,066	76.49	<0.001
Error	16	23,649	1478		
Lack-of-fit	10	16,071	1607	1.27	0.4
Pure Error	6	7578	1263		
Total	30	1,606,567			

[a] Coefficient of determination (R^2) = 98.53%; adjusted R^2 = 97.24%; [b] DF, degree of freedom; SS, sum of squares; MS, mean square.

Table 4. Significance of the model parameters.

Term	Parameter Estimate	Standard Error	*t*-Value	*p*-Value [a]
β_0	1245.0	14.5	85.68	0.000 [a]
β_1	−15.61	7.85	−1.99	0.064
β_2	−0.06	7.85	−0.01	0.994
β_3	18.60	7.85	2.37	0.03 [a]
β_4	3.45	7.85	0.44	0.667
β_{11}	−182.99	7.19	−25.45	0.000 [a]
β_{22}	−105.02	7.19	−14.61	0.000 [a]
β_{33}	−108.43	7.19	−15.08	0.000 [a]
β_{44}	−107.22	7.19	−14.91	0.000 [a]
β_{12}	−38.60	9.61	−4.02	0.001 [a]
β_{13}	−14.21	9.61	−1.48	0.159
β_{14}	16.62	9.61	1.73	0.103
β_{23}	−7.06	9.61	−0.73	0.473
β_{24}	35.26	9.61	3.67	0.002 [a]
β_{34}	12.10	9.61	1.26	0.226

[a] $p < 0.05$ indicates that the model terms are significant.

3.2. Combined Influence of Culture Conditions

Figure 1 illustrates the mutual influence of reducing sugar concentration and urea concentration on the astaxanthin yield while other factors were maintained at a central level. At a specific concentration of urea, increasing the concentration of reducing sugar in molasses hydrolysate resulted in a significantly enhanced astaxanthin yield. This is because the yeast strain required sugars as a carbon source for its growth and metabolism [27]. Yeast cells consume and convert glucose and other reducing sugars to intermediates such as ethanol and acetic acid through their metabolic pathways. Acetyl CoA (a precursor for carotenoid biosynthesis) was then produced from ethanol by alcohol dehydrogenase [16] and facilitated the synthesis of carotenoids (including astaxanthin). However, after reaching the highest astaxanthin yield, a further increase in the reducing sugar concentration caused a reduction in astaxanthin yield. This might be because the high molasses hydrolysate concentration increased the sugar osmotic pressure, which inhibited cell growth and promoted the synthesis of other energetic substances (e.g., protein), instead of astaxanthin to resist to environmental stress, thus lowering astaxanthin production [28]. Moreover, several by-products (e.g., 5 hydroxymethylfurfural) might be formed during the hydrolysis step and their presence at a high concentration in the culture medium could inhibit cell

growth and astaxanthin production [29,30]. Similarly, at a given concentration of reducing sugar, the astaxanthin yield increased with an increasing concentration of urea, reached the highest level, and then reduced [28]. Excess urea resulted in a reduction in the carbon-to-nitrogen ratio, thus suppressing the cell growth and synthesis of secondary pigments, including astaxanthin. Therefore, a sufficient carbon-to-nitrogen ratio is required for the cell growth and biosynthesis of astaxanthin by *R. toruloides* G17. In this work, the highest astaxanthin yield was obtained in the middle-range concentrations of both the reducing sugar and urea.

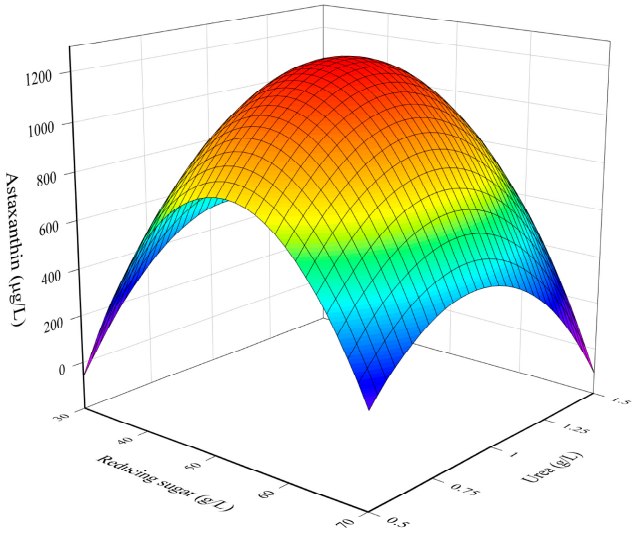

Figure 1. Combined effect of reducing sugar concentration and urea concentration on the astaxanthin yield.

Figure 2 illustrates the combined influence of reducing sugar concentration and $MgSO_4 \cdot 7H_2O$ concentration on astaxanthin yield. At a given reducing sugar concentration, the astaxanthin yield increased and reached its highest level when the $MgSO_4 \cdot 7H_2O$ concentration increased. However, high concentrations of $MgSO_4 \cdot 7H_2O$ (>5.5 mg/mL) resulted in a decrease in astaxanthin yield. This was because this salt is essential for cell growth and, when present in sufficient quantities, it promotes the carotenogenesis process in the cells. However, an excess of $MgSO_4$ suppressed cell growth and astaxanthin biosynthesis, thus reducing the astaxanthin yield [31,32].

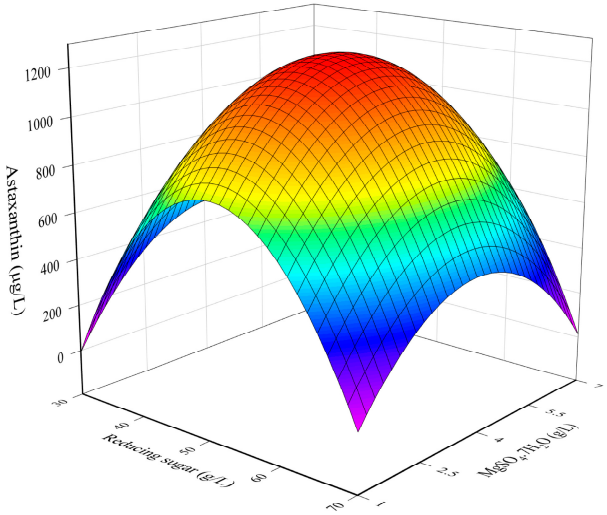

Figure 2. Combined effect of reducing sugar concentration and $MgSO_4 \cdot 7H_2O$ concentration on the astaxanthin yield.

Figure 3 displays the mutual effects of the urea concentration and inoculum ratio on the astaxanthin yield, while other factors were maintained at their central levels. At a specific urea concentration, increasing the inoculum ratio led to an enhanced astaxanthin yield. This result indicated that the initial concentration of *R. toruloides* G17 inoculum strongly affected astaxanthin production. The highest astaxanthin yield was obtained with the culture containing high inoculum ratios. This could be because these cultures shortened the lag phase, efficiently consuming and converting nutrients into their biomass and astaxanthin accumulation, thus enhancing astaxanthin yield. This result was similar to previous studies which demonstrated that when the inoculum ratio is under or over the limit threshold, it could lead to a poor growth rate of microorganisms [33]. Studies have reported that the lower the inoculum ratio, the longer it takes to pass the log phase [34], thus reducing the accumulation of secondary metabolites, which are mainly formed in the stationary phases [14].

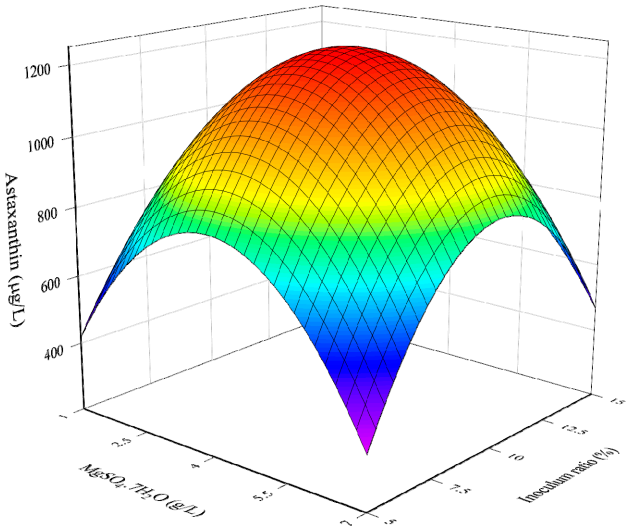

Figure 3. Combined effect of $MgSO_4 \cdot 7H_2O$ concentration and inoculum ratio on the astaxanthin yield.

3.3. Determination of Optimal Culture Conditions

The model Equation (6) was solved to predict the optimal conditions for maximizing the astaxanthin yield. The optimal conditions were determined to be a reducing sugar concentration of 49.39 g/L, urea concentration of 1.00 g/L, $MgSO_4 \cdot 7H_2O$ concentration of 4.15 g/L, and inoculum ratio of 10.05%, with a corresponding astaxanthin yield of 1246.19 μg/L. To validate this prediction, *R. toruloides* G17 was grown under the same optimized conditions to produce astaxanthin. The experimental astaxanthin content was 1262.08 ± 14.58 μg/L, which was consistent with the prediction. This finding demonstrated that the RSM model was successfully developed to establish the relationship between culture conditions and astaxanthin yield in the cultivation of *R. toruloides* G17 in molasses hydrolysate-based medium. The cultivation of *R. toruloides* G17 in waste molasses-based medium produced a higher astaxanthin yield than *Phaffia rhodozyma* (639.6 μg/L) [35] and *Spirulina platensis* (38 μg/L) [36]. Therefore, *R. toruloides* G17 is promising for further applications.

3.4. Astaxanthin Purification

Astaxanthin extract was loaded onto a silica gel column and eluted with n-hexane:acetone (4:1, *v*/*v*) for purification (Figure 4a). Subsequently, three fractions (A1, A2, and A3) were obtained and subjected to TLC analysis. As shown in Figure 4b, high purity astaxanthin was found in fraction A2 with an R_f value of 0.29, which was the same R_f value as that of the astaxanthin standard. In addition, liquid chromatography-mass spectrometry (LC-MS) was used to further identify the extracted astaxanthin. GC–MS analysis showed that the extracted astaxanthin and astaxanthin standard had the same retention time (5.849–5.865 min) and mass to charge ratio [*m*/*z* 597.39 (M+)] (Figures S1 and S2, Supplementary Material).

Therefore, this fraction was used for further experiments to investigate its antioxidant and anticancer activities.

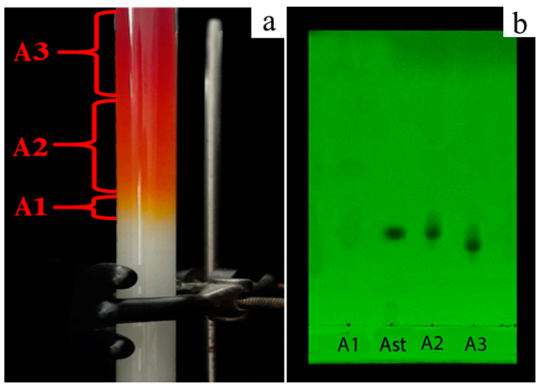

Figure 4. Purification of astaxanthin using silica gel column chromatography (**a**) and TLC analysis of astaxanthin fractions (**b**). A1: fraction 1; A2: fraction 2; A3: faction 3; and Ast: astaxanthin standard.

3.5. Antioxidant Activity of Astaxanthin

There has been a growing interest in using natural antioxidants for preventing diseases and promoting health [37,38]. As a result, various natural sources have been studied for producing antioxidant compounds [39,40]. In recent years, astaxanthin has increasingly received attention from academia and industry since it exhibits potent antioxidant activity. In the current study, the antioxidant activity of astaxanthin produced by mutated *R. toruloides* G17 was investigated using the DPPH scavenging activity assay and compared to that of α-tocopherol (a positive control). The DPPH reaction mechanism is based on hydrogen donation, whereby DPPH compounds (deep-violet) are captured by antioxidant compounds, releasing hydrogen radicals to form stable the molecules of DPPH-H (colorless or pale-yellow) [41,42]. As shown in Figure 5a, the produced astaxanthin strongly scavenged DPPH radicals at low concentrations. Notably, the astaxanthin exhibited 123.6-fold higher DPPH scavenging activity (IC_{50} of 0.97 ± 0.01 μg/mL) than α-tocopherol (IC_{50} of 119.91 ± 0.91 μg/mL). In addition, the DPPH radical scavenging activity of the astaxanthin obtained in this work was found to be higher than that obtained from other natural sources, as illustrated in Table 5. It could be because astaxanthin from different sources has variations in terms of its chiral structure, thus affecting its antioxidant activity [43]. Astaxanthin has multiple isomeric forms including geometric isomers, stereoisomers, esterified, and free forms [44]. Studies have reported that the biological activity of astaxanthin varies among its isomeric forms [43,44]. The (3S, 3′S)-isomers have been found to exhibit higher antioxidant activity than (3R, 3′R) and (3R, 3′S) astaxanthins [43]. The high antioxidant activity of astaxanthin can be explained by the keto group in astaxanthin activating the hydroxyl group and consequently promoting hydrogen transfer to the peroxyl radicals [45]. Hence, astaxanthin effectively inhibited free radicals. This finding indicated that astaxanthin produced by the mutated *R. toruloides* G17 is a promising antioxidant agent for further applications.

Table 5. DPPH scavenging activity of astaxanthin from different sources.

Sources	IC_{50} Value (μg/mL)	References
R. toruloides	0.97	This study
Shrimp waste	17.50	[41]
P. longirostris	6.30	[46]
Scylla serrata	805.84	[47]
H. pluvialis	15.39–56.25	[48]
Phaffia rhodozyma	31.79	[49]
Chlorella zofingiensis	1040–2930	[50]

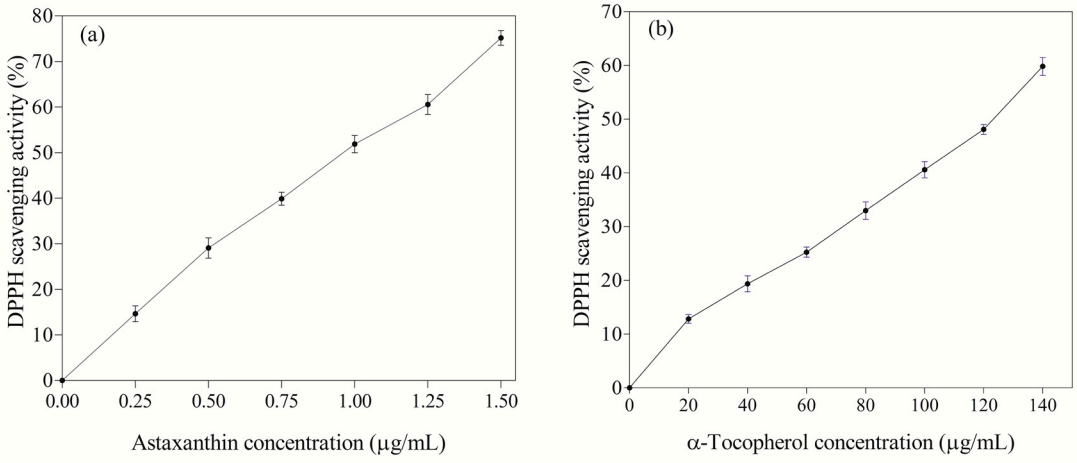

Figure 5. DPPH scavenging activity of (**a**) astaxanthin and (**b**) α-tocopherol.

3.6. Anticancer Activity of Astaxanthin

This study examined the cytotoxicity of astaxanthin produced by *R. toruloides* G17 in one control (HK2) and three cancer cell lines (MCF7, A549, and HeLa). Astaxanthin significantly suppressed the proliferation of MCF7, A549, and Hela cell lines in a dose-dependent manner while exerting less damage to the HK2 cells. The anticancer activity of astaxanthin was found to be lower than that of Cisplatin, known to be one of the most effective chemotherapeutic anticancer agents, but it still exhibited cytotoxicity against A549, MCF7, and HeLa cells with IC_{50} values of 56.38 ± 4.1 μg/mL, 55.60 ± 2.64 μg/mL, and 69.07 ± 2.4 μg/mL, respectively (Table 6). The cytotoxicity of astaxanthin obtained in this work was comparable to that previously observed for astaxanthin from other sources. Kim et al. [51] reported the cytotoxicity of astaxanthin (Sigma-Aldrich) in two gastric cancer cell lines, KATO-III and SNU-1, with the IC_{50} values of >100 μg/mL. Ramamoorthy et al. [52] investigated the effect of astaxanthin (purified fraction) extracted from the microalgae *H. pluvialis* and observed a significant reduction in cell viability (about 50%) at an astaxanthin concentration of 50 μM. The present work suggests that astaxanthin produced by *R. toruloides* G17 is a potential antitumor agent.

Table 6. IC_{50} values of anticancer activity of astaxanthin.

Sample	IC_{50} Value (μg/mL)			
	MCF7	**A549**	**HeLa**	**HK2**
Astaxanthin	55.60 ± 2.6	56.38 ± 4.1	69.07 ± 2.4	111.34 ± 1.4
Cisplatin	21.68 ± 0.8	2.4 ± 0.4	6.8 ± 0.9	1.8 ± 0.7

Data are expressed as mean ± SD of three independent experiments.

4. Conclusions

This study reported the production of astaxanthin from waste molasses by *R. toruloides* G17. RSM was employed to optimize the culture conditions for maximizing the astaxanthin yield. Through RSM, the optimal culture conditions (concentration of reducing sugar of 49.39 g/L, urea concentration of 1.00 g/L, $MgSO_4 \cdot 7H_2O$ concentration of 4.15 g/L, and inoculum ratio of 10.05%) were obtained, with the highest astaxanthin yield of 1262.08 ± 14.58 μg/L. The produced astaxanthin exhibited potent antioxidant activity (IC_{50} of 0.97 ± 0.01 μg/mL) and anticancer activity against the three cancer cell lines, HeLa, A549, and MCF7, with IC_{50} values of 69.07 ± 2.4 μg/mL, 55.60 ± 2.64 μg/mL, and 56.38 ± 4.1 μg/mL, respectively. This study suggests that *R. toruloides* G17 is a promising strain for the production of bioactive astaxanthin using low-cost molasses as a source of carbon and micronutrients. The produced astaxanthin may have applications as a nutraceutical or pharmaceutical grade antioxidant or antitumor agent.

Supplementary Materials: The following supporting information can be downloaded at: https://www.mdpi.com/article/10.3390/fermentation9020148/s1, Figure S1: Liquid chromatography-mass spectrometry (LC-MS) chromatogram of astaxanthin standard; Figure S2: Liquid chromatography-mass spectrometry (LC-MS) chromatogram of extracted astaxanthin.

Author Contributions: Conceptualization, T.N.T., H.C.N., D.-N.N. and C.J.B.; methodology, T.N.T., H.C.N., C.-H.S. and D.-C.P.; validation, N.-T.T., T.-A.T., D.-C.P. and T.N.T.; formal analysis, T.N.T. and H.C.N.; investigation, T.N.T., N.-T.T. and T.-A.T.; resources, H.C.N., C.J.B. and D.-N.N.; writing—original draft preparation, H.C.N.; writing—review and editing, C.J.B.; visualization, T.N.T. and H.C.N.; supervision, D.-N.N., H.C.N. and C.J.B.; project administration, D.-N.N.; funding acquisition, D.-N.N. All authors have read and agreed to the published version of the manuscript.

Funding: This research received no external funding.

Institutional Review Board Statement: Not applicable.

Informed Consent Statement: Not applicable.

Data Availability Statement: The data are available from the corresponding author upon request.

Conflicts of Interest: The authors declare no conflict of interest.

References

1. Faraone, I.; Sinisgalli, C.; Ostuni, A.; Armentano, M.F.; Carmosino, M.; Milella, L.; Russo, D.; Labanca, F.; Khan, H. Astaxanthin anticancer effects are mediated through multiple molecular mechanisms: A systematic review. *Pharmacol. Res.* **2020**, *155*, 104689. [CrossRef]
2. Demirel, P.B.; Tuna, B.G. Anticancer properties of astaxanthin: A molecule of great promise. In *Global Perspectives on Astaxanthin*; Academic Press: Cambridge, MA, USA, 2021; pp. 427–445.
3. Fakhri, S.; Abbaszadeh, F.; Dargahi, L.; Jorjani, M. Astaxanthin: A mechanistic review on its biological activities and health benefits. *Pharmacol. Res.* **2018**, *136*, 1–20. [CrossRef]
4. Kurashige, M.; Okimasu, E.; Inoue, M.; Utsumi, K. Inhibition of oxidative injury of biological membranes by astaxanthin. *Physiol. Chem. Phys. Med. NMR* **1990**, *22*, 27–38.
5. Davinelli, S.; Nielsen, M.E.; Scapagnini, G. Astaxanthin in skin health, repair, and disease: A comprehensive review. *Nutrients* **2018**, *10*, 522. [CrossRef]
6. Higuera-Ciapara, I.; Felix-Valenzuela, L.; Goycoolea, F. Astaxanthin: A review of its chemistry and applications. *Crit. Rev. Food Sci. Nutr.* **2006**, *46*, 185–196. [CrossRef]
7. Zhou, P.; Li, M.; Shen, B.; Yao, Z.; Bian, Q.; Ye, L.; Yu, H. Directed coevolution of β-carotene ketolase and hydroxylase and its application in temperature-regulated biosynthesis of astaxanthin. *J. Agric. Food Chem.* **2019**, *67*, 1072–1080. [CrossRef]
8. Asker, D. Isolation and characterization of a novel, highly selective astaxanthin-producing marine bacterium. *J. Agric. Food Chem.* **2017**, *65*, 9101–9109. [CrossRef]
9. Kamath, B.S.; Srikanta, B.M.; Dharmesh, S.M.; Sarada, R.; Ravishankar, G.A. Ulcer preventive and antioxidative properties of astaxanthin from *Haematococcus pluvialis*. *Eur. J. Pharmacol.* **2008**, *590*, 387–395. [CrossRef]
10. Schmidt, I.; Schewe, H.; Gassel, S.; Jin, C.; Buckingham, J.; Hümbelin, M.; Sandmann, G.; Schrader, J. Biotechnological production of astaxanthin with *Phaffia rhodozyma*/*Xanthophyllomyces dendrorhous*. *Appl. Microbiol. Biotechnol.* **2011**, *89*, 555–571. [CrossRef]
11. Chang, M.X.; Xiong, F. Astaxanthin and its effects in inflammatory responses and inflammation-associated diseases: Recent advances and future directions. *Molecules* **2020**, *25*, 5342. [CrossRef]
12. Nguyen, K.D. Astaxanthin: A Comparative Case of Synthetic vs. Natural Production. Chemical and Biomolecular Engineering Publications and Other Works. Available online: http://trace.tennessee.edu/utk_chembiopubs/94 (accessed on 5 January 2023).
13. Wen, Z.; Zhang, S.; Odoh, C.K.; Jin, M.; Zhao, Z.K. *Rhodosporidium toruloides*—A potential red yeast chassis for lipids and beyond. *FEMS Yeast Res.* **2020**, *20*, foaa038. [CrossRef]
14. Tran, T.N.; Ngo, D.H.; Tran, Q.T.; Nguyen, H.C.; Su, C.H.; Ngo, D.N. Enhancing astaxanthin biosynthesis by *Rhodosporidium toruloides* mutants and optimization of medium compositions using response surface methodology. *Processes* **2020**, *8*, 497. [CrossRef]
15. Wu, Y.H.; Yang, J.; Hu, H.Y.; Yu, Y. Lipid-rich microalgal biomass production and nutrient removal by *Haematococcus pluvialis* in domestic secondary effluent. *Ecol. Eng.* **2013**, *60*, 155–159. [CrossRef]
16. Tran, T.N.; Quang-Vinh, T.; Huynh, H.T.; Hoang, N.S.; Nguyen, H.C.; Dai-Nghiep, N. Astaxanthin production by newly isolated *Rhodosporidium toruloides*: Optimization of medium compositions by response surface methodology. *Not. Bot. Horti Agrobot.* **2019**, *47*, 320–327. [CrossRef]
17. Dalsasso, R.R.; Pavan, F.A.; Bordignon, S.E.; de Aragão, G.M.F.; Poletto, P. Polyhydroxybutyrate (PHB) production by *Cupriavidus necator* from sugarcane vinasse and molasses as mixed substrate. *Process Biochem.* **2019**, *85*, 12–18. [CrossRef]

18. Yew, G.Y.; Khoo, K.S.; Chia, W.Y.; Ho, Y.C.; Law, C.L.; Leong, H.Y.; Show, P.L. A novel lipids recovery strategy for biofuels generation on microalgae *Chlorella cultivation* with waste molasses. *J. Water Process Eng.* **2020**, *38*, 101665. [CrossRef]
19. Yew, G.Y.; Puah, B.K.; Chew, K.W.; Teng, S.Y.; Show, P.L.; Nguyen, T.H.P. *Chlorella vulgaris* FSP-E cultivation in waste molasses: Photo-to-property estimation by artificial intelligence. *Chem. Eng. J.* **2020**, *402*, 126230. [CrossRef]
20. Kundu, S.; Panda, T.; Majumdar, S.; Guha, B.; Bandyopadhyay, K. Pretreatment of Indian cane molasses for increased production of citric acid. *Biotechnol. Bioeng.* **1984**, *26*, 1114–1121. [CrossRef]
21. Miller, G.L. Use of dinitrosalicylic acid reagent for determination of reducing sugar. *Anal. Chem.* **1959**, *31*, 426–428. [CrossRef]
22. Prasertsung, I.; Aroonraj, K.; Kamwilaisak, K.; Saito, N.; Damrongsakkul, S. Production of reducing sugar from cassava starch waste (CSW) using solution plasma process (SPP). *Carbohydr. Polym.* **2019**, *205*, 472–479. [CrossRef]
23. An, G.H.; Bielich, J.; Auerbach, R.; Johnson, E.A. Isolation and characterization of carotenoid hyperproducing mutants of yeast by flow cytometry and cell sorting. *Nat. Biotechnol.* **1991**, *9*, 70–73. [CrossRef]
24. Fang, T.J.; Cheng, Y.S. Improvement of astaxanthin production by *Phaffia rhodozyma* through mutation and optimization of culture conditions. *J. Ferment. Bioeng.* **1993**, *75*, 466–469. [CrossRef]
25. Sánchez-Moreno, C. Methods used to evaluate the free radical scavenging activity in foods and biological systems. *Food Sci. Technol. Inter.* **2002**, *8*, 121–137. [CrossRef]
26. Pham, D.C.; Chang, Y.C.; Lin, S.R.; Fuh, Y.M.; Tsai, M.J.; Weng, C.F. FAK and S6K1 inhibitor, neferine, dually induces autophagy and apoptosis in human neuroblastoma cells. *Molecules* **2018**, *23*, 3110. [CrossRef]
27. Koschwanez, J.H.; Foster, K.R.; Murray, A.W. Sucrose utilization in budding yeast as a model for the origin of undifferentiated multicellularity. *PLoS Biol.* **2011**, *9*, e1001122. [CrossRef]
28. Nguyen, H.C.; Su, C.H.; Yu, Y.K.; Huong, D.T.M. Sugarcane bagasse as a novel carbon source for heterotrophic cultivation of oleaginous microalga *Schizochytrium* sp. *Ind. Crop. Prod.* **2018**, *121*, 99–105. [CrossRef]
29. Zeng, Y.; Bian, D.; Xie, Y.; Jiang, X.; Li, X.; Li, P.; Zhang, Y.; Xie, T. Utilization of food waste hydrolysate for microbial lipid and protein production by *Rhodosporidium toruloides* Y2. *J. Chem. Technol. Biotechnol.* **2017**, *92*, 666–673. [CrossRef]
30. Howard, J.; Rackemann, D.W.; Bartley, J.P.; Samori, C.; Doherty, W.O. Conversion of sugar cane molasses to 5-hydroxymethylfurfural using molasses and bagasse-derived catalysts. *ACS Sustain. Chem. Eng.* **2018**, *6*, 4531–4538. [CrossRef]
31. Fang, C.J.; Ku, K.L.; Lee, M.H.; Su, N.W. Influence of nutritive factors on C50 carotenoids production by *Haloferax mediterranei* ATCC 33500 with two-stage cultivation. *Bioresour. Technol.* **2010**, *101*, 6487–6493. [CrossRef]
32. Varmira, K.; Habibi, A.; Bahramian, E.; Jamshidpour, S. Progressive agents for improvement of carotenogenesis in *Rhodotorula rubra*. *J. Adv. Food Sci. Technol.* **2016**, *3*, 70–78.
33. Narayanaswamy, S. *Plant Cell and Tissue Culture*; Tata McGraw-Hill Education: New York, NY, USA, 1994.
34. Ling, O.S.; Kiong, A.L.P.; Hussein, S. Establishment and optimisation of growth parameters for cell suspension cultures of *Ficus deltoidea*. *Am. Eurasian J. Sustain. Agric.* **2008**, *2*, 38–49.
35. Xie, H.; Zhou, Y.; Hu, J.; Chen, Y.; Liang, J. Production of astaxanthin by a mutant strain of *Phaffia rhodozyma* and optimization of culture conditions using response surface methodology. *Ann. Microbiol.* **2014**, *64*, 1473–1481. [CrossRef]
36. An, J.; Gao, F.; Ma, Q.; Xiang, Y.; Ren, D.; Lu, J. Screening for enhanced astaxanthin accumulation among *Spirulina platensis* mutants generated by atmospheric and room temperature plasmas. *Algal Res.* **2017**, *25*, 464–472. [CrossRef]
37. Nguyen, H.C.; Nguyen, H.N.T.; Huang, M.Y.; Lin, K.H.; Pham, D.C.; Tran, Y.B.; Su, C.H. Optimization of aqueous enzyme-assisted extraction of rosmarinic acid from rosemary (*Rosmarinus officinalis* L.) leaves and the antioxidant activity of the extract. *J. Food Process. Preserv.* **2021**, *45*, e15221. [CrossRef]
38. Nguyen, H.C.; Kuan-Hung, L.; Huang, M.Y.; Chi-Ming, Y.; Tin-Han, S.; Hsiung, T.C.; Yen-Chang, L.; Fun-Chi, T. Antioxidant activities of the methanol extracts of various parts of Phalaenopsis orchids with white, yellow, and purple flowers. *Not. Bot. Horti Agrobot.* **2018**, *46*, 457–465. [CrossRef]
39. Do, T.H.; Huynh, T.D.; Vo, K.A.; Nguyen, K.A.; Cao, T.S.; Nguyen, K.N.; Nguyen, H.A.H.; Nguyen, T.T.T.; Le, N.P.N.; Truong, D.H. Saponin-rich fractions from *Codonopsis javanica* root extract and their in vitro antioxidant and anti-enzymatic efficacy. *J. Food Process. Preserv.* **2022**, *46*, e16113. [CrossRef]
40. Truong, D.H.; Nguyen, D.H.; Ta, N.T.A.; Bui, A.V.; Do, T.H.; Nguyen, H.C. Evaluation of the use of different solvents for phytochemical constituents, antioxidants, and in vitro anti-inflammatory activities of *Severinia buxifolia*. *J. Food Qual.* **2019**, *2019*, 8178294. [CrossRef]
41. Chintong, S.; Phatvej, W.; Rerk-Am, U.; Waiprib, Y.; Klaypradit, W. In vitro antioxidant, antityrosinase, and cytotoxic activities of astaxanthin from shrimp waste. *Antioxidants* **2019**, *8*, 128. [CrossRef]
42. Santos-Sánchez, N.F.; Salas-Coronado, R.; Villanueva-Cañongo, C.; Hernández-Carlos, B. Antioxidant compounds and their antioxidant mechanism. In *Antioxidants*; IntechOpen: London, UK, 2019; Volume 10, pp. 1–29.
43. Sun, J.; Yan, J.; Dong, H.; Gao, K.; Yu, K.; He, C.; Mao, X. Astaxanthin with different configurations: Sources, activity, post-modification and application in foods. *Curr. Opin. Food Sci.* **2023**, *49*, 100955. [CrossRef]
44. Ambati, R.R.; Moi, P.S.; Ravi, S.; Aswathanarayana, R.G. Astaxanthin: Sources, extraction, stability, biological activities and its commercial applications—A review. *Mar. Drugs* **2014**, *12*, 128–152. [CrossRef]
45. Naguib, Y.M. Antioxidant activities of astaxanthin and related carotenoids. *J. Agric. Food Chem.* **2000**, *48*, 1150–1154. [CrossRef] [PubMed]

46. Abdelmalek, B.E.; Sila, A.; Ghlissi, Z.; Taktak, M.A.; Ayadi, M.A.; Bougatef, A. The influence of natural astaxanthin on the formulation and storage of marinated chicken steaks. *J. Food Biochem.* **2016**, *40*, 393–403. [CrossRef]
47. Karnila, R.; Edison; Ramadhani, N.R. Antioxidant activity of astaxanthin flour extract of mud crab (*Scylla serrata*) with different acetone concentrations. In Proceedings of the IOP Conference Series: Earth and Environmental Science 2021, Pekanbaru, Indonesia, 10–11 September 2020; p. 012047.
48. Tan, Y.; Ye, Z.; Wang, M.; Manzoor, M.F.; Aadil, R.M.; Tan, X.; Liu, Z. Comparison of different methods for extracting the astaxanthin from *Haematococcus pluvialis*: Chemical composition and biological activity. *Molecules* **2021**, *26*, 3569. [CrossRef] [PubMed]
49. Cheng, X.Y.; Xiong, Y.J.; Yang, M.M.; Zhu, M.J. Preparation of astaxanthin mask from *Phaffia rhodozyma* and its evaluation. *Process Biochem.* **2019**, *79*, 195–202. [CrossRef]
50. Sun, Z.; Liu, J.; Zeng, X.; Huangfu, J.; Jiang, Y.; Wang, M.; Chen, F. Astaxanthin is responsible for antiglycoxidative properties of microalga *Chlorella zofingiensis*. *Food Chem.* **2011**, *126*, 1629–1635. [CrossRef]
51. Kim, J.H.; Park, J.J.; Lee, B.J.; Joo, M.K.; Chun, H.J.; Lee, S.W.; Bak, Y.T. Astaxanthin inhibits proliferation of human gastric cancer cell lines by interrupting cell cycle progression. *Gut Liver* **2016**, *10*, 369. [CrossRef]
52. Ramamoorthy, K.; Raghunandhakumar, S.; Anand, R.; Paramasivam, A.; Kamaraj, S.; Nagaraj, S.; Ezhilarasan, D.; Lakshmi, T.; Dua, K.; Chellappan, D.K. Anticancer effects and lysosomal acidification in A549 cells by astaxanthin from *Haematococcus lacustris*. *Bioinformation* **2020**, *16*, 965. [CrossRef] [PubMed]